

AD-A055 187 AIR FORCE INST OF TECH WRIGHT-PATTERSON AFB OHIO SCH--ETC F/G 6/18  
USE OF A METAL-NITRIDE-OXIDE-SEMICONDUCTOR AS THE DETECTOR FOR --ETC(U)  
MAR 78 R G FRAASS

UNCLASSIFIED

AFIT/GNE/PH/78M-3

NL

1 OF 1  
AD  
A055 187



END  
DATE  
FILMED

7-78

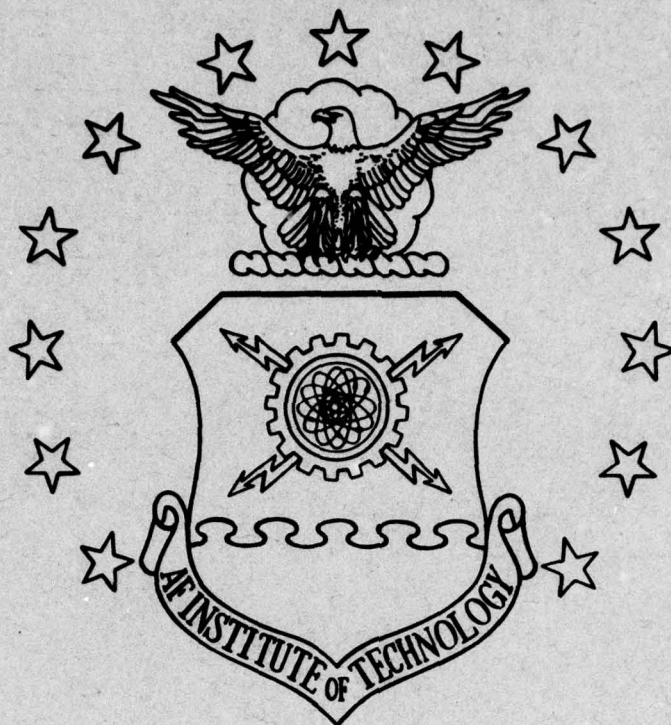
DDC

AD A 055187

AD No. \_\_\_\_\_  
DDC FILE COPY

FOR FURTHER TRAN

1  
B.S.



DDC  
RECEIVED  
JUN 19 1978  
E

UNITED STATES AIR FORCE  
AIR UNIVERSITY  
AIR FORCE INSTITUTE OF TECHNOLOGY  
Wright-Patterson Air Force Base, Ohio

CIVIL ENGINEERING SCHOOL

DISTRIBUTION STATEMENT A

Approved for public release;  
Distribution Unlimited

78 06 13 045

AFIT/GNE/PH/78M-3

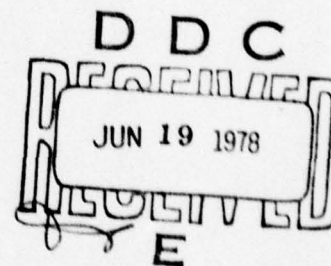
①

USE OF A  
METAL-NITRIDE-OXIDE-SEMICONDUCTOR  
AS THE DETECTOR FOR A  
RADIATION DOSIMETER

THESIS

GNE/PH/78M-3

Ronald G. Fraass  
Capt USAF



Approved for public release; distribution unlimited

78 06 13 045



USE OF A  
METAL-NITRIDE-OXIDE-SEMICONDUCTOR  
AS THE DETECTOR FOR A  
RADIATION DOSIMETER

THESIS

Presented to the Faculty of the School of Engineering  
of the Air Force Institute of Technology  
Air University  
in Partial Fulfillment of the  
Requirements for the Degree of  
Master of Science

ACCESSION for		
NTIS	White Section	<input checked="" type="checkbox"/>
DDC	Buff Section	<input type="checkbox"/>
UNANNOUNCED		<input type="checkbox"/>
JUSTIFICATION.....		
BY.....		
DISTRIBUTION/AVAILABILITY CODES		
Dist.	AVAIL. and/or SPECIAL	
A		

by  
Ronald G. Fraass, B.S.  
Capt                      USAF  
Graduate Nuclear Engineering  
March 1978



### Preface

This report is the summary of my investigations into the use of a Metal-Nitride-Oxide-Semiconductor as the detector for a high dose level radiation dosimeter. I terminated my research after completing a partially automated dosimeter. Further work is needed to bring the dosimeter to the production stage. A small microprocessor should be added to allow a direct readout of radiation dose. At its present stage of development the dosimeter reading is used in conjunction with a graph to give a value of radiation dosage.

This research was sponsored by the Transient Radiation Effects Branch of the Air Force Weapons Laboratory (AFWL/ELT), Kirtland AFB, New Mexico.

For their encouragement and support, I am indebted to my advisors, Dr. George John and Dr. Richard Hagee. Roger Tallon of the AFWL was instrumental in the procurement of the MNOS devices and in initial circuit design. The technicians of the AFIT Physics Department assisted in circuit fabrication.

The essential support for this entire project came from my wife, Linda, and our two children. Without their understanding and love this dosimeter would still be only a possibility.

Ronald G. Fraass

## Contents

	Page
Preface . . . . .	ii
List of Figures . . . . .	v
List of Tables . . . . .	vi
Abstract . . . . .	vii
I. Introduction . . . . .	1
MIS Dosimetry . . . . .	2
Scope of the Problem . . . . .	3
Approach . . . . .	3
II. MNOS Theory . . . . .	5
MNOS . . . . .	5
Operation . . . . .	7
Threshold Voltage . . . . .	7
Conduction State . . . . .	7
Writing . . . . .	9
Clear . . . . .	9
Mechanism . . . . .	11
Time Effects . . . . .	11
Radiation Effects . . . . .	13
Theory . . . . .	13
Read-Disturb . . . . .	19
III. Equipment and Procedures . . . . .	21
Radiation Facilities . . . . .	21
MNOS Transistors . . . . .	22
Test Fixture . . . . .	22
Threshold Detection Circuitry . . . . .	23
Read Pulse . . . . .	25
Operation of the Test Circuit . . . . .	25
Clear . . . . .	26
Write . . . . .	26
Reading . . . . .	28
Experimental Method . . . . .	28
Standardized Testing Procedure . . . . .	30
Saturation . . . . .	30
Selected Threshold Voltage . . . . .	31

	Page
IV. Results . . . . .	32
Time Dependence . . . . .	32
Radiation and Time Dependence . . . . .	33
Dosimetry Data . . . . .	35
Theoretical Curve Fit . . . . .	35
Precision . . . . .	37
Total Dose Effects . . . . .	37
Dosimetry . . . . .	37
Permanent Radiation Damage . . . . .	39
V. Conclusions and Recommendations . . . . .	42
Conclusions . . . . .	42
Recommendations . . . . .	44
Bibliography . . . . .	46
Vita . . . . .	48



List of Tables

<u>Table</u>		<u>Page</u>
I	Relative Precision of Dosimeter . . . . .	38
II	Dose Rate Calculations at Low Dose Rate . . . . .	38
III	Dose Rate Calculations at High Dose Rate . . . . .	38

Abstract

A method of radiation dosimetry using a Metal-Nitride-Oxide-Semiconductor (MNOS) device as the detector was developed and partially evaluated.

The MNOS devices are capable of measuring doses from 10 k rads to 4 M rads. Repeatability of observations indicates a precision of  $\pm 1\%$  of total dose from 200 k rads to 4 M rads (Si). Dosage in rads is obtained by reference to a calibrated source exposure rate and not to dose absorbed within the dosimeter. A  $\text{Co}^{60}$  source was used for all radiation testing.

Schematics are given for some of the circuits tested. Determination of dosage from the system is indirect and requires the use of a calibration curve. Each dosimeter must be calibrated from a known source. Direct readout of dose is suggested by use of a microprocessor.

Exposure to  $2 \times 10^7$  rads did not degrade performance. Devices eventually failed due to charge migration from the large integrated circuit chip on which they were fabricated. Discrete, non-stepped gate MNOS transistors are recommended.

USE OF A METAL-NITRIDE-OXIDE-SEMICONDUCTOR  
AS THE DETECTOR FOR A RADIATION DOSIMETER

I. Introduction

A direct readout method of radiation dosimetry was desired for certain experimental work at the Air Force Weapons Laboratory (AFWL), Kirtland AFB, NM (Ref 8). The experimental work required determination of radiation dosages in semiconductor materials which were irradiated with a pulsed X-ray or electron beam machine. These irradiation methods require that the target materials be in a vacuum chamber. Most standard dosimeters, as the Thermoluminescence dosimeter (Ref 7:397-409) or Ceric Sulphate dosimeter (Ref 3), would need to be removed from the target chamber after each dose to permit them to be read to determine the radiation dosage. Removal of the dosimeter from the target chamber between radiation exposures meant a delay of several hours between pulses. This lengthy delay included time for reading the dosimeter and time to again achieve the desired vacuum in the target chamber. If an accurate dosimetry technique which permitted direct electrical readout of dose were available, the delay between radiation tests could be greatly reduced.

The AFWL suggested that one possibility for such a dosimeter might be based on the use of a Metal-Nitride-Oxide-Semiconductor (MNOS) transistor (Ref 8). Therefore, the purpose of this experimental study was to determine the feasibility of using an MNOS transistor as the detector in a radiation dosimeter.



### MIS Dosimetry

The use of an MNOS as a dosimeter follows from dosimetry methods using similar devices. The MNOS transistor is a member of the Metal-Insulator-Semiconductor (MIS) family. Other better known members are the Metal-Oxide-Semiconductor-Field-Effect Transistor (MOSFET) and the Metal-Oxide-Semiconductor Capacitor (MOSC). Use of the MIS family of devices as dosimeters is possible since radiation produces measurable effects in each of these devices. Radiation dosimeters have been designed using both the MOSFET (Ref 1) and the MOSC (Ref 4).

A problem with both the MOSFET and MOSC dosimeters is the semi-permanence of the radiation effects in both (Ref 6:1270). This problem prevents individual calibration of a given dosimeter. Lack of individual calibration limits precision to  $\pm 5\%$  when devices from a single semiconductor wafer are used. If devices from different wafers are used for calibration, the precision drops to  $\pm 20\%$  (Ref 4:351).

An alternative to the MOSC and MOSFET is offered by the MNOS. Its characteristics are similar to those of the MOSFET with one major difference. The electrical characteristics of the MNOS, which are altered by radiation, can be returned to their pre-irradiation values through the application of a proper electrical signal (Ref 12). Since radiation effects are not permanent in the MNOS, a dosimeter incorporating an MNOS could be individually calibrated to permit high precision.

A possible further advantage of the MNOS is its greater hardness to radiation effects. The MOSFETS used by Poch and Holmes-Siedle showed saturation dose effects at  $4 \times 10^4$  rads (Si) (Ref 1). Studies of the radiation hardness of MNOS memory arrays (Ref 12:186) have shown

that saturation effects did not occur until  $3 \times 10^6$  rads (Si). Consequently, an MNOS dosimeter could measure doses nearly two orders of magnitude higher than the MOSFET dosimeter.

### Scope of the Problem

The primary purpose of this experimental study was to determine the feasibility of using an MNOS transistor as a radiation dosimeter. If the MNOS were shown to be usable as a dosimeter, the design and characteristics of an MNOS dosimeter were to be studied.

The scope of this problem was limited to the study of a group of MNOS transistor devices both before and after their exposure to  $\text{Co}^{60}$  radiation, and the study of an MNOS dosimetry method which requires manual operation and graphical determination of radiation dosage. Study of the manual dosimetry system included determination of minimum measurable dose, maximum measurable dose, and precision. Final design of a fully automatic MNOS dosimeter was considered to be beyond the scope of this study.

### Approach

Verification of the MNOS dosimetry concept began with a study of the characteristics of the MNOS transistor. The general results of that study are shown in Chapter II. Once the general theory of the MNOS devices was understood, electrical circuitry had to be designed to allow testing of the MNOS devices. Chapter III includes a description of the devices tested, the experimental setup, and the testing procedures used on the MNOS devices. Since the test circuit was able to measure the effects of radiation on the MNOS devices, it was, in effect, a manual

## II. MNOS Theory

Much of the theory concerning the MNOS detector deals with its use as an electronic memory. The MNOS was developed as an attempt to produce a better Metal-Oxide-Semiconductor-Field-Effect-Transistor (MOSFET). One of the principle characteristics of the MOSFET is a fixed threshold voltage. When the early MNOS devices were tested for threshold voltage, unexpected results were obtained. The threshold voltage was found to be variable and dependent upon the electric field previously applied from gate to substrate. This variable threshold voltage gave rise to the use of the device as an electronic memory.

Radiation degradation of the information stored in an MNOS memory unit led to its consideration as a radiation detector. In order to design an MNOS detector, a general understanding of the characteristics of the device is required. This chapter describes the basic MNOS device, its operation, charge transport mechanisms, effects on stored charge by time and radiation, and the read-disturb effect.

### MNOS

The MNOS transistor is an Insulated-Gate-Field-Effect-Transistor (IGFET), similar to the MOSFET. However, it has a double layer of insulator material. Figure 1 is a diagram of a p-channel enhancement-mode MNOS transistor. The substrate, 200 microns thick, is lightly doped n-type silicon. The source and drain are both heavily doped p-type regions. A gate region is above and between the source and drain.



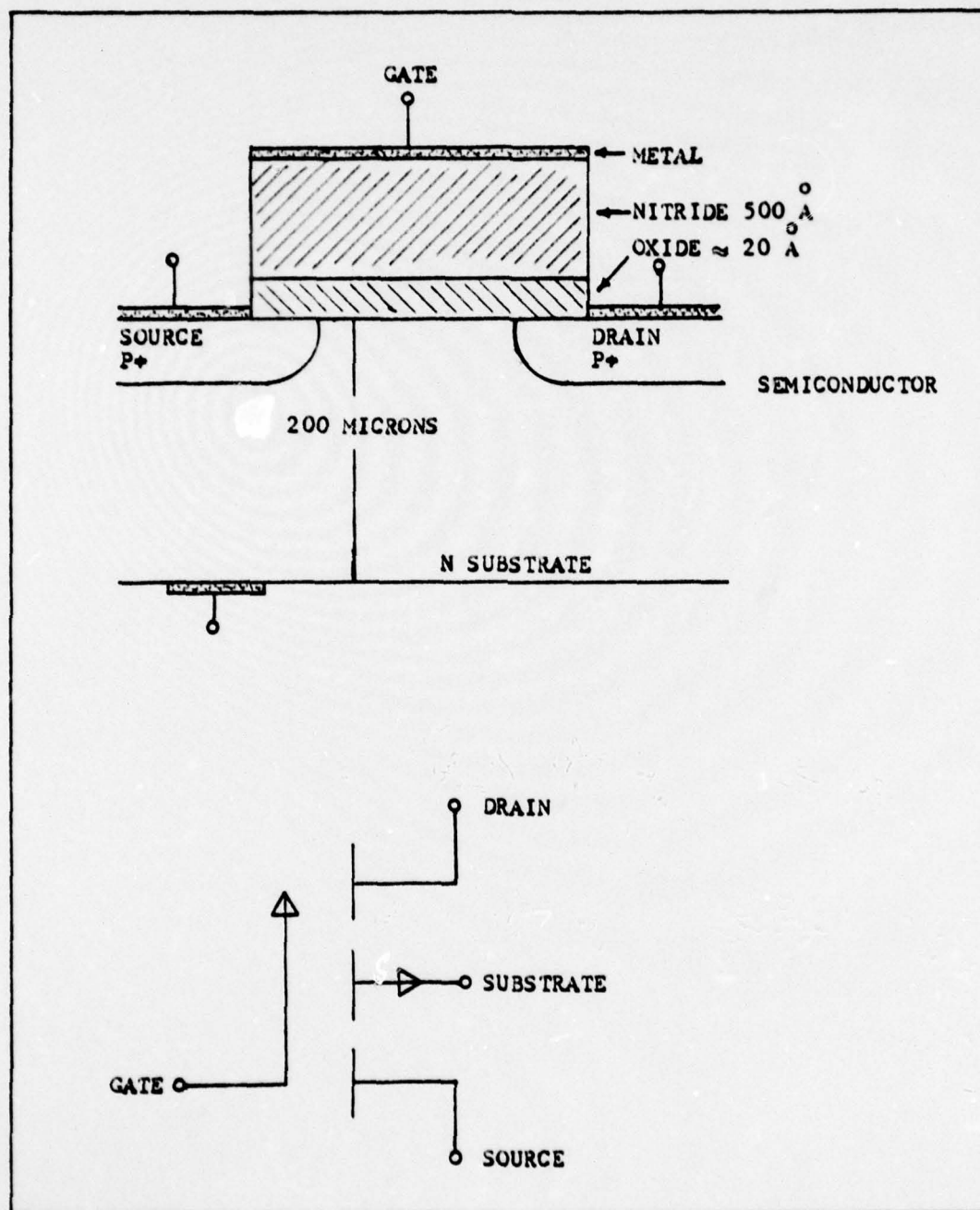


Fig. 1. P-Channel Enhancement Mode MNOS Transistor and Symbol

The gate region consists of  $20 \text{ \AA}$  of  $\text{SiO}_2$  covered by  $500 \text{ \AA}$  of  $\text{Si}_3\text{N}_4$ . Metalized contacts are provided for electrical connections to the drain, source, gate, and substrate.

### Operation

The operation of an MNOS transistor is dependent on the voltage applied to the gate and drain. For the p-channel enhancement-mode device in Fig. 2, current will flow between source and drain when a sufficiently negative voltage is applied from gate to substrate ( $V_{GS}$ ). The negative voltage on the gate pulls holes up to the silicon/silicon-dioxide interface. The holes in the formerly n-type material form a conduction channel between the source and drain. This channel permits a current to flow from source to drain.

Threshold Voltage. A variable threshold voltage ( $V_T$ ) is a characteristic of an MNOS which distinguishes it from an MOS transistor. Threshold voltage is defined as the value of  $V_{GS}$  which permits a defined amount of source-drain current ( $I_{SD}$ ) to flow. For this experiment  $V_T$  was defined as the value of  $V_{GS}$  which resulted in a total source-drain current equal to leakage current plus ten microamperes. Fig. 3 is a generalized set of  $V_{GS}$  versus  $I_{SD}$  curves for an MNOS. It can be seen that the values of the leakage current ( $I_{SD0}$ ) and  $V_T$  are dependent on the conduction state of the device.

Conduction State. The MNOS may be described as being in either a high conduction state or a low conduction state. The  $V_{GS}$  versus  $I_{SD}$  curve can lie anywhere between the two extremes of saturated high-conductance and saturated low-conductance. Typical values of  $V_T$  might be  $-0.4$  volts in the high-conduction state and  $-11$  volts in the

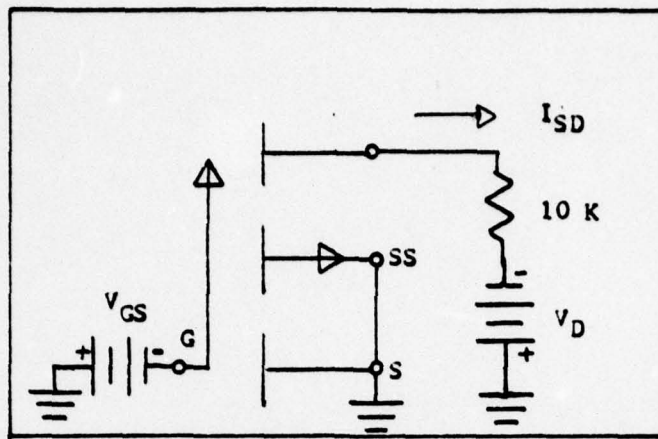


Fig. 2. Biasing for an MNOS Transistor

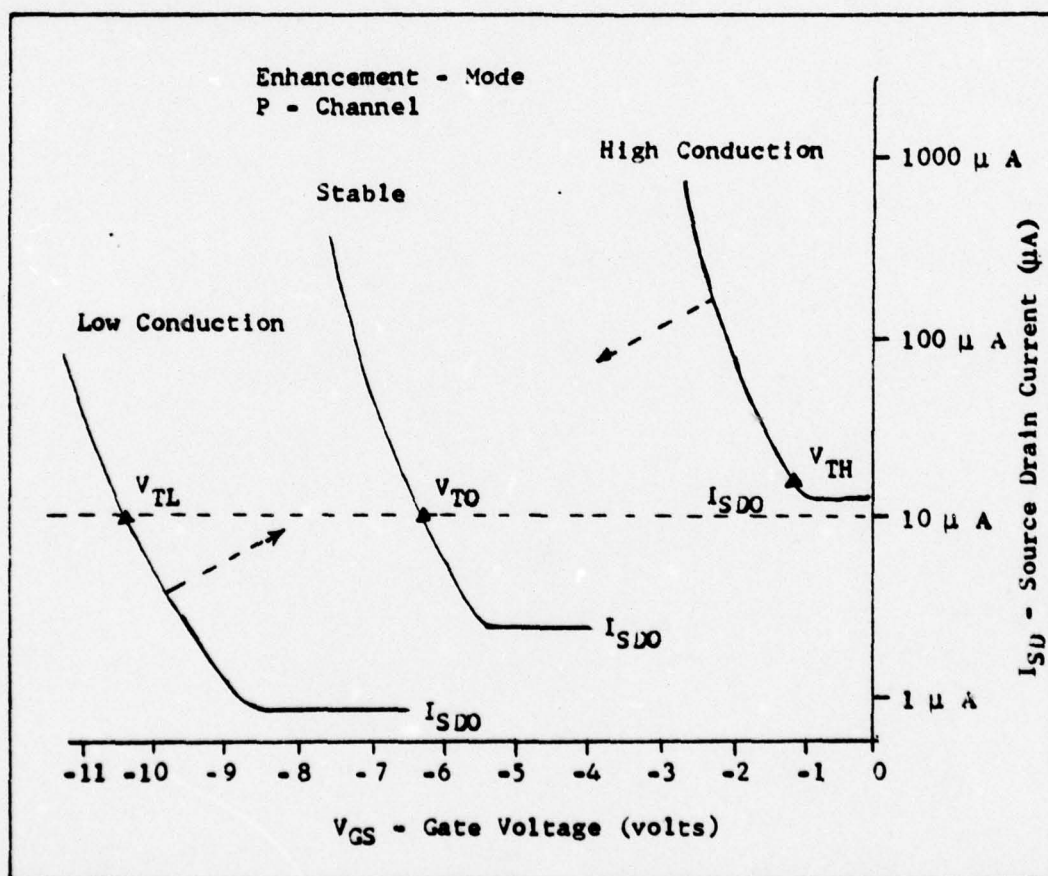


Fig. 3. Generalized Curves for Source Drain Current ( $I_{SD}$ ) Versus Gate Voltage ( $V_{GS}$ )



low-conduction state. The magnitude of threshold voltage in the high-conduction state,  $V_{TH}$ , is always less than the magnitude of the threshold voltage in the low-conduction state,  $V_{TL}$ . The third curve in Fig. 3 shows the point  $V_{TO}$ . After sufficient time, the  $I_{DS}$  versus  $V_{GS}$  curves move from either saturated condition to that middle curve.  $V_{TO}$  may be called a stable threshold voltage because it does not change with time. The difference between  $V_T$  in a low and high-conduction state depends upon the amount and polarity of charge which is stored in the device at the silicon-nitride/silicon-dioxide interface.

Writing. The placing of additional negative charges at the interface is defined as writing. A saturate write pulse for a p-channel enhancement mode MNOS is a positive  $V_{GS}$  pulse. It must be of sufficient magnitude and duration to put the device into a saturated high-conduction state. During the application of the write pulse, as seen in Fig. 4, electrons penetrate the thin oxide by a tunneling process and enter deep traps in the silicon-nitride near the boundary of the nitride and oxide layers. Saturation occurs when the field across the oxide due to trapped charge equals the field due to the externally applied  $V_{GS}$ . Once the write pulse is removed, as shown in Fig. 5, the stored negative charge draws holes from the substrate to the substrate/oxide interface. These holes partially open a conduction path from the source to the drain. This conduction path increases the leakage current and decreases the magnitude of the threshold voltage.

Clear. During a clear operation, as shown in Fig. 6, a negative  $V_{GS}$  pulse is applied. This causes trapping of holes in the nitride at the nitride/oxide interface. After the clear pulse ends, the trapped

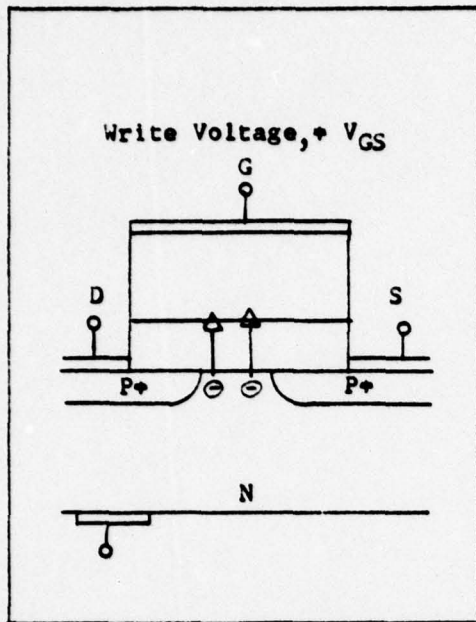


Fig. 4. Application of  $+V_{GS}$  Write Voltage

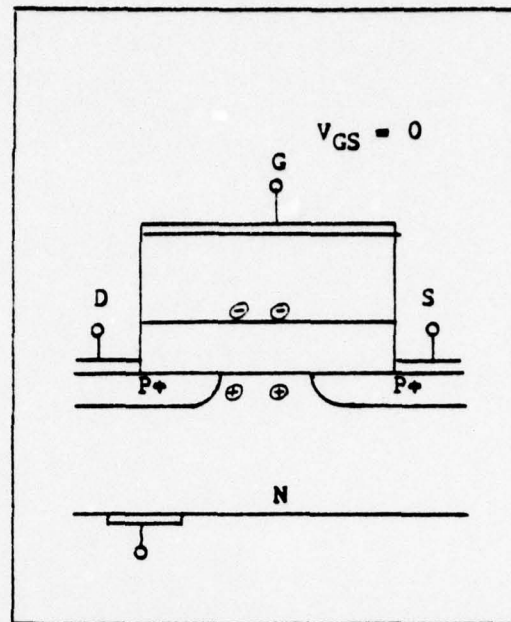


Fig. 5. Trapped Electrons After End of Write Pulse

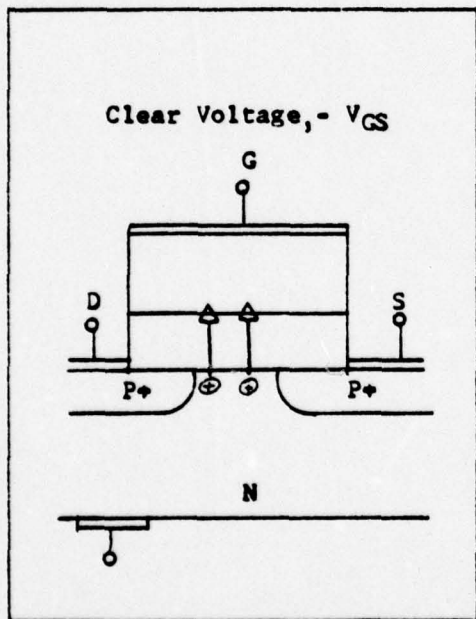


Fig. 6. Application of  $-V_{GS}$  Clear Voltage

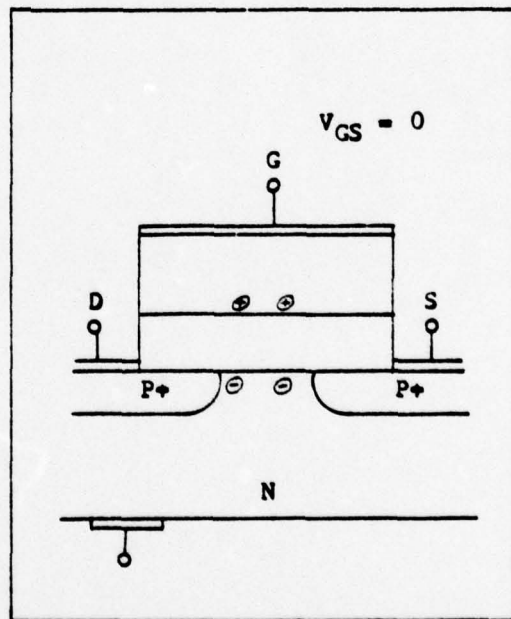


Fig. 7. Trapped Holes After End of Clear Pulse

holes pull free electrons to the surface in the substrate as shown in Fig. 7. The excess electrons effectively block the conduction path between source and drain. Leakage current is therefore reduced and the magnitude of  $V_T$  increases.

### Mechanism

A more detailed discussion of the mechanisms of charge transport in and characteristics of the MNOS is given by Frohman-Bentchkowsky (Ref 2) and by Lundstrom and Swensson (Ref 9). Lundstrom and Swensson indicate that modified Fowler-Nordheim tunneling may be the mechanism for transport of charge through the oxide when high external fields are applied and the oxide is thin (Ref 9:829). Fowler-Nordheim tunneling is based on the quantum physics principle of tunneling. The Fowler-Nordheim expression is modified by Lundstrom and Swensson to include specific probabilities for transmission of carriers through the oxide and nitride.

However, charge transport continues after the removal of  $V_{GS}$ . This continued charge transport is controlled by the internal fields due to the trapped charge carriers. The charge transport, due to recombination, tends to neutralize the stored charge after sufficient time.

### Time Effects

The changes in  $V_T$  with time are seen in Fig. 8. The threshold voltage can be seen to be linear in  $\log(t)$  at least out to  $10^3$  minutes. The curve for a device initially in the low-conduction state is similar (Ref 12:63). The dependence of  $V_T$  on stored charge seen from the time effects is also the basis for the primary radiation effects in MNOS.



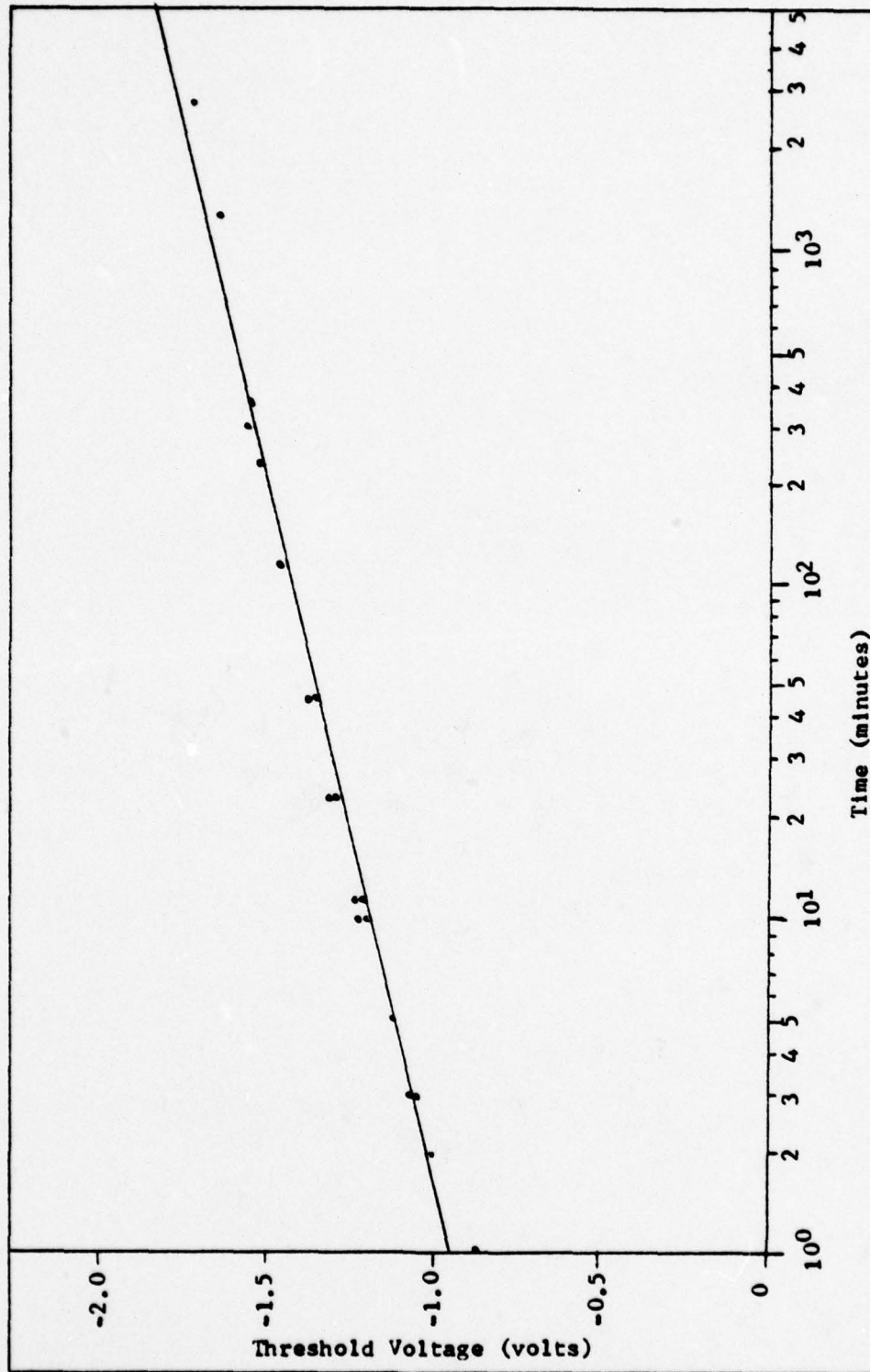


Fig. 8. MNOS Threshold Voltage Versus Time

### Radiation Effects

Radiation induced changes in an MNOS are due primarily to the effects of electron-hole pairs, produced by the radiation. Incident gamma radiation (Cobalt 60) produces Compton electrons which in turn produce electron-hole pairs. These free charge carriers move through the oxide under the influence of the internal electric fields produced by the trapped carriers in the silicon-nitride. They then recombine with the trapped carriers to reduce the stored charge and cause the threshold voltage to change.

Theory. An empirical equation has been developed which relates the threshold voltage in an MNOS transistor to absorbed radiation dose. The theory leading to the equation is shown in Appendix I of Ref 12. The development proceeds from the basic relationships between applied field, space charge, and current in an insulator; and then assumes a radiation induced change in space charge based on ohmic conduction in the insulators. A portion of that development is presented here.

The nitride and oxide layers of an MNOS gate are modeled as a two-layer insulator as in Fig. 9. A thin layer of charge  $\sigma$  is assumed to lie in a plane at the nitride-oxide interface. The relationship between  $\sigma$ , the nitride field  $E_n$ , the oxide field  $E_o$ , and the applied voltage  $V_G$  is as follows:

$$E_n x_n + E_o x_o = V_{GS} \quad (1)$$

$$\epsilon_o E_o - \epsilon_n E_n = \sigma \quad (2)$$

where  $\epsilon_n$  and  $\epsilon_o$  are the dielectric permittivities of the nitride and oxide layers, and  $x_n$  and  $x_o$  are the thicknesses.

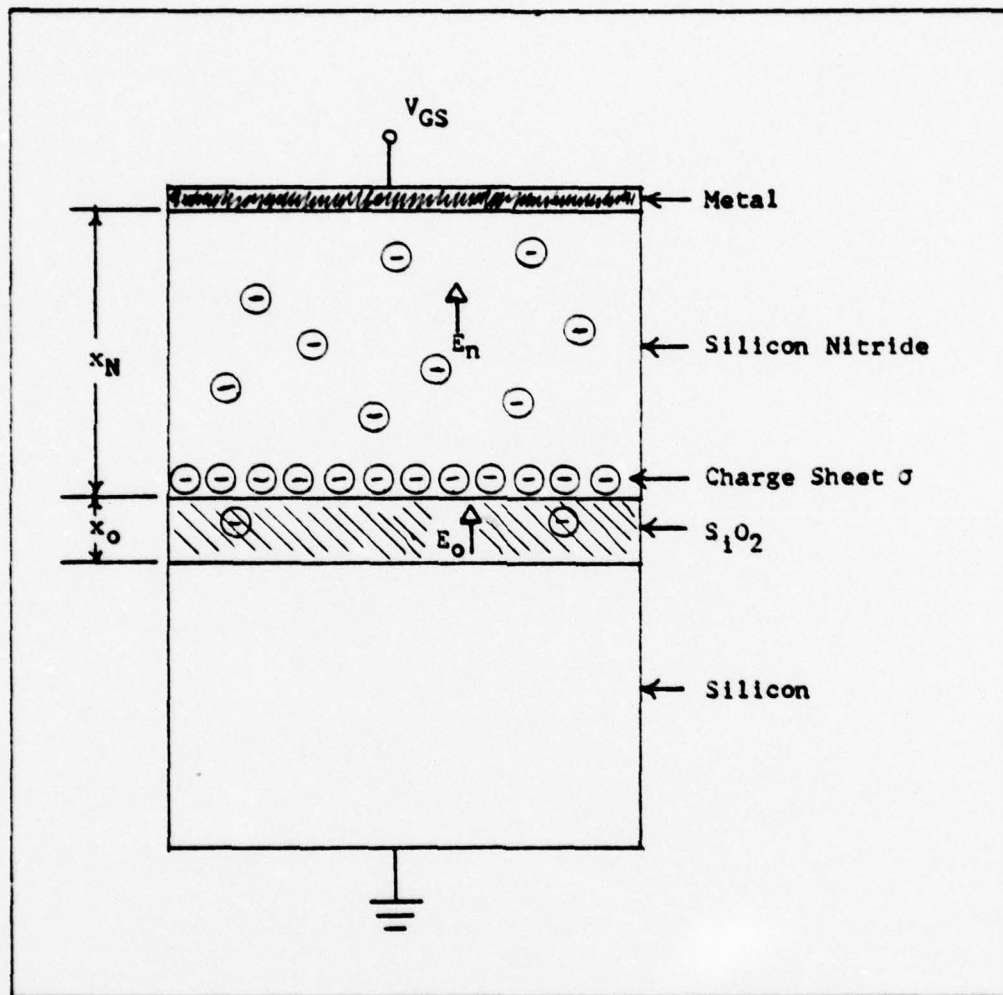


Fig. 9. MNOS Gate Region (From Ref 12:187)



It is assumed that the value of  $\sigma$  at the interface is responsible for changes in  $V_{FB}$ , the flatband voltage. The flatband voltage is that value of  $V_{GS}$  which results in  $E_o = 0$ . Putting this relationship into Eqs (1) and (2) yields

$$V_{FB} = -\sigma \frac{x_n}{\epsilon_n} \quad (3)$$

Equations (1), (2), and (3) then may be solved for  $E_n$  and  $E_o$ :

$$E_o = \gamma \epsilon_n (V_{GS} - V_{FB}) \quad (4)$$

$$E_n = \gamma \epsilon_o (V_{GS} + \beta V_{FB}) \quad (5)$$

where  $\gamma = (\epsilon_n x_o + \epsilon_o x_n)^{-1}$  and  $\beta = \epsilon_n x_o / \epsilon_o x_n$ . Eqs (4) and (5) are valid for  $E_o$  and  $E_n$  at any instant of time. To determine  $V_{FB}$  as a function of time requires the use of the equation of current continuity for the system.

$$\epsilon_o \frac{dE_o}{dt} + j_o = \epsilon_n \frac{dE_n}{dt} + j_n \quad (6)$$

From Eq (6), which states that the sum of the displacement and particle currents is the same in both layers,

$$\tau = \int_{V_{FB}^i}^{V_{FB}^f} \frac{\epsilon_o dE_o - \epsilon_n dE_n}{j_n - j_o} \quad (7)$$

When Eq (2) is differentiated, combined with Eq (3), and substituted into Eq (7), one obtains

$$\tau = \frac{\epsilon_n}{x_n} \int_{V_{FB}^i}^{V_{FB}^f} - \frac{(dV_{FB})}{j_n - j_o} \quad (8)$$

Eq (8) gives the time to change from  $V_{FB}^i$ , the initial flatband voltage to  $V_{FB}^f$ , the final flatband voltage. The result holds for any two-layer insulator system on a nondegenerate semiconductor. If the denominator is changed to  $j_n + j_o$ , the equation also holds for discharging (removing stored charges). The value of  $V_{FB}$  as a function of time can be determined if Eq (8) is integrated using equations for  $j_o$  and  $j_n$  and the proper limits.

The effects of radiation enter into Eq (8) through the current density terms,  $j_n$  and  $j_o$ . It is assumed that at sufficiently high dose rates the generation of charge carriers will depend primarily upon the radiation dose instead of bulk generation rates. In such a case, the net carrier density will not depend on applied field. This will give rise to a form of ohmic conduction across the oxide and nitride layers.

Net carrier density, considering recombination, and under irradiation is given by:

$$n = g\tau \text{ and } g = k\dot{R} \quad (9)$$

where  $g$  is the electron-hole pair generation rate and  $\tau$  the effective (and constant) lifetime. In this case  $g$  is assumed proportional by a constant  $k$  to the dose rate  $\dot{R}$  in rads/second. For ohmic conduction

$$1/\rho = ne\mu = e\tau\mu = ek\dot{R}\tau\mu \quad (10)$$

where  $1/\rho$  is the conductivity in (A/V)-cm,  $\mu$  the mobility in  $\text{cm}^2/\text{V-s}$  and  $e$  the number of coulombs per carrier. The conductivity is proportional to dose rate  $\dot{R}$  and a lumped material constant  $\alpha = ek\tau\mu$  giving

$$1/\rho = \alpha\dot{R} \quad (11)$$

To complete the development of current density, there is Ohm's law

$$j = E/\rho = \alpha \dot{R} E \quad (12)$$

where  $j$  is current density in  $A/cm^2$  and  $E$  is the field in  $V/cm$ .

Assuming that the current density due to radiation is much larger than the normal current density, the current density due to radiation can be substituted into Eq (8) as follows:

$$j_{nR} = \alpha_n \dot{R} E_n \quad (13)$$

$$j_{oR} = \alpha_o \dot{R} E_o \quad (14)$$

where the subscript  $R$  indicates current density due to radiation.

Substituting for  $E_n$  and  $E_o$  in Eqs (13) and (14) by using Eqs (4) and (5)

$$j_{nR} = \alpha_n \dot{R} \epsilon_o (V_{GS} + \beta V_{FB}) \quad (15)$$

$$j_{oR} = \alpha_o \dot{R} \epsilon_n (V_{GS} - V_{FB}).$$

Substitution of Eqs (15) and (16) into (8) using the current densities due to radiation leads to

$$-BR = \int_{V_{FB}}^{V_{FB}^f} \frac{1}{AV_{GS} + V_{FB}} \frac{dV_{FB}}{V_{FB}} \quad (16)$$

$$\text{where: } B = (\alpha_n \epsilon_o \beta + \alpha_o \epsilon_n) \gamma x_n / \epsilon_n \quad (17)$$

$$R = \dot{R} t, \text{ the total dose, and} \quad (18)$$

$$A = (\alpha_n \epsilon_o - \alpha_o \epsilon_n) / (\alpha_n \epsilon_o \beta + \alpha_o \epsilon_n) \quad (19)$$



After integration and rearrangement, this results in

$$V_{FB} = V_{FB}^i \exp(-BR) + AV_{GS} [\exp(-BR) - 1] \quad (20)$$

This expression describes the change of  $V_{FB}$  as a combination of an exponential decay of stored charge and an exponential build up of new charges at the interface due to an applied voltage  $V_{GS}$ .

Since the flatband voltage and threshold voltage can be related by

$$V_{FB} = V_T - V_{TO} \quad (21)$$

Eq (20) can be rewritten as

$$V_T = V_{TO} + (V_T^i - V_{TO}) \exp(-BR) + AV_{GS} [\exp(-BR) - 1] \quad (22)$$

Changes were made to Eq (22) for the purposes of this study. The term multiplied by the constant A was set equal to zero since the value of  $V_{GS}$  was at zero during the experimental tests except for determinations of the threshold voltage. The second change involved replacing the threshold voltage  $V_T$  and the stable threshold voltage  $V_{TO}$  by  $\Delta V_T$  and  $\Delta V_{TMAX}$ .

$$\Delta V_T = \Delta V_{TMAX} [1 - \exp(-BR)] \quad (23)$$

where  $\Delta V_T^i = 0$ , and the terms  $\Delta V_T$  and  $\Delta V_{TMAX}$  represent the change in threshold voltage for a given dose of radiation R.  $\Delta V_{TMAX}$  represents the maximum threshold voltage shift given an infinite radiation dosage. It corresponds to the stable threshold voltage  $V_{TO}$ . Eq (23) should fit the experimental data from an MNOS when change in threshold voltage is graphed versus radiation dosage.

Marraffino et al used Eq (20) to fit data from three MNOS devices with different oxide thicknesses and nitride trap densities. In each case the empirically determined value of the constant B was found to be  $8 \times 10^{-7} \text{ rads}^{-1}$  (Ref 12:18,19). The value of B was considered to be relatively invariant due to the relative invariance of the conductance properties of the different oxide layers in the three device types (Ref 12:19).

#### Read-Disturb

A final characteristic of the MNOS which must be considered is the read-disturb effect (Ref 10:2-22). Reading is the operation of applying a variable  $V_{GS}$  to an MNOS to determine its threshold voltage. Any externally applied field ( $V_{GS}$ ) will tend to disturb the amount of stored charge in the nitride. To prevent read-disturb effects, the read pulse-width must be kept much less than the write or clear pulse-widths. A possible mechanism for the read-disturb effect is trap-assisted charge injection as described by Swensson (Ref 13).

An example of a shift in threshold voltage due to read-disturb effect can be seen in Fig.10. The write pulse for this device was 100 milliseconds at +15 volts. The output can be seen to have decreased during the 10 millisecond read pulse. The output voltage is read across a 10 K resistor and indicates the changes in source drain current. The output would have remained constant had there been no read-disturb effects.

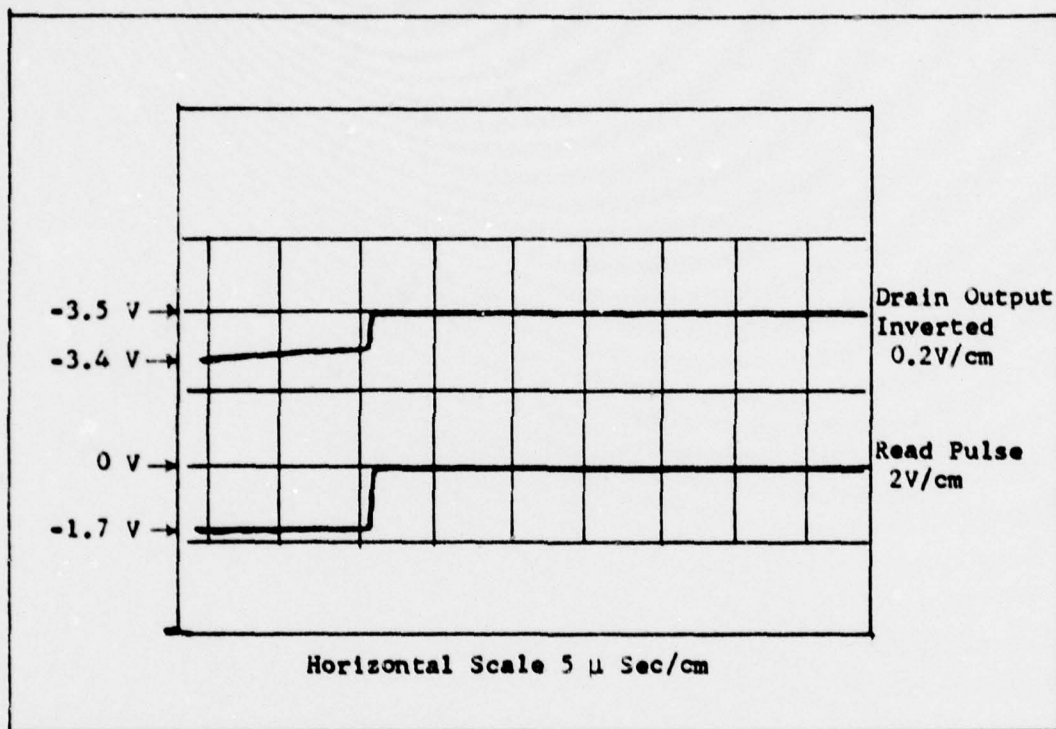


Fig. 10. Read Disturb Effect on Threshold Voltage



### III. Equipment and Procedures

This chapter on equipment and procedures provides information on the radiation facilities used, the test devices and circuitry, and the experimental procedures used to obtain the data on the MNOS dosimeter. In the second section of this chapter, minimal information on the specific structure of the MNOS transistors is given due to restrictions on proprietary information. The final two sections, on experimental method and standardized testing procedure, are critical to the reproducibility of experimental results.

#### Radiation Facilities

Two  $\text{Co}^{60}$  sources were used for the radiation tests in this study. Most of the testing was done in the North Gamma Irradiation Facility (North GIF) at Sandia Laboratories, Albuquerque, New Mexico. The North GIF permits a dose rate of nearly  $6 \times 10^4$  rads (Si)/minute at the center of the source array. Lower dose rates are available at different points throughout the cell.

A second radiation source was the Gamma Irradiation Facility at the Air Force Institute of Technology (AFIT), Wright-Patterson AFB, Ohio. It was limited to a dose of  $5 \times 10^4$  rads (Si)/hour. The AFIT GIF only had provision for irradiation in the center of its source array.

Different experimental positions in the North GIF have been previously calibrated in units of absorbed dose, rads ( $\text{H}_2\text{O}$ ). Conversion factors are given for rads (Si). Consequently, calibration of a

dosimeter can be made directly in rads by reference to the given exposure rate of the source.

### MNOS Transistors

The MNOS transistors used in this study are test transistors which were fabricated along with several other circuits on a single silicon chip. The chips are packaged in 14-pin ceramic flat packs. However, leads were available only for the MNOS test transistors. Due to the restricted number of leads on a flat pack, there was some commonality of substrate, source, and gate leads. This permitted each of the six transistors on a chip to have a separate drain connection.

Standard MNOS production techniques were used to make the transistors. The dimensions given in Fig. 1 are approximately those of the transistors used in this experimental study. The experimental devices were prepared by Sandia Laboratories, Albuquerque, New Mexico, in August 1977.

Non-stepped gate MNOS transistors, as in Fig. 1, were the primary test devices. However, there were also MNOS transistors with either a single or double stepped gate structure available on the MNOS device. None of these gate structures had diode protection. This lack of protection required extra care in handling. Any discharge of static electricity into the unprotected gates could punch through the thin oxide, destroying the device.

### Test Fixture

Electrical contact to a selected transistor was provided by a test fixture. It permitted easy switching between the transistors on a

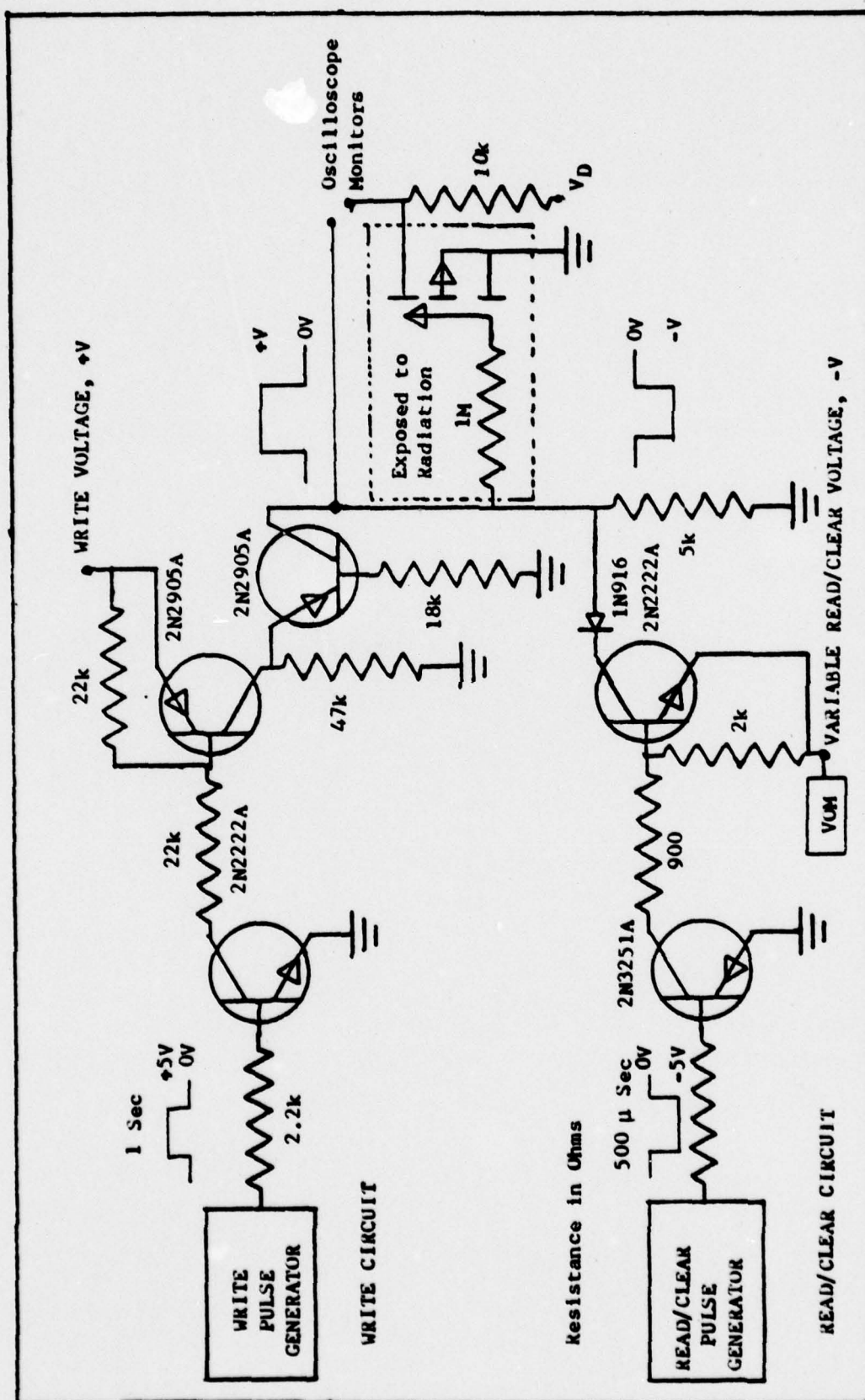
single device or between different devices. The devices were held in flat-pack sockets which were attached to a 15 contact plug board. A device change therefore required only an exchange of plug boards. The plug boards mated with a socket in a small aluminum chassis box.

The chassis box had a series of eight SPDT switches which permitted selection of the transistor to be tested. One side of each switch was connected to ground. The other side was connected to either the gate or drain outputs on the chassis box. This design allowed a selected gate and drain to be connected to the test circuit while the other drains and gate were held at ground. In addition, a 1 M resistor was connected in series with the gate output. The resistor served to protect the transistor being tested from excess current which might damage its gate. The chassis box also grounded all source and substrate leads.

#### Threshold Detection Circuitry

A simple electronic circuit, shown in Fig. 11, was used to inject variable voltage and variable pulse-width signals into the gate of an MNOS under test. Roger Tallon, of the Air Force Weapons Laboratory, Kirtland AFB, New Mexico, designed the original circuit. It had been used to test early MNOS devices for radiation hardness. The circuit was monitored at two places with an oscilloscope. The gate signal was monitored prior to the MNOS to determine voltage and pulse width. A second monitor point was the drain output of the MNOS. The drain was connected by a 10K precision resistor to the drain power supply  $V_D$ . Any change in current through the resistor was seen on the scope as a change in voltage.





The circuit delivers either a positive (write) or a negative (read/clear) pulse into the gate of the transistor being tested. The amplitude of the pulse is varied through the use of variable power supplies for the read/clear and write circuits. Provision for varying the pulse width is provided by external pulse generators which trigger the test circuitry.

Read Pulse. The measurement of the amplitude of the read pulse is critical to the use of the circuit for reading the threshold of an MNOS. Best precision was obtained by reading the value of the read/clear power supply with a digital voltmeter. Although the full read/clear supply voltage does not appear at the gate, the reduction in voltage is nearly constant. It can be seen from Fig. 11 that most of the reduction is in the forward bias voltage of the diode which protects the read/clear circuit. For the circuit shown, this voltage reduction was 0.65 volts. The values of threshold voltage reported in this paper all reflect the added 0.65 volts. True threshold voltage as previously defined would equal the stated value minus 0.65 volts.

The test circuit is connected to the test fixture with coaxial cable. The circuit is capable of driving 25 feet of 50 ohm cable with minimal signal loss. Only two cables are required between the circuit and test fixture. One cable carries the gate signal and the other carries the drain output signal.

#### Operation of the Test Circuit

The test circuit can be used for three operations on the MNOS being tested. First, it can be used to clear previously stored negative charge with a negative pulse. Second, it can be used to write, the

addition of negative stored charge, with a positive pulse. And, third, it can be used to read the threshold voltage with a negative pulse. The read/clear section of the circuit provides both of the necessary negative pulses. The two operations of reading and clearing only differ in pulse width and amplitude.

Clear. Clearing the MNOS being tested requires a large, -20 volts, negative pulse of long duration, 1 second. The clear circuit is triggered by a -5 volt pulse from an external pulse generator. Pulse width of the clear pulse is also determined by the external pulse generator. The amplitude of the clear pulse is adjustable by selection of the power supply voltage to the read/clear circuit.

Fig. 12 shows the results of a clear operation. The output at the drain is driven hard to ground since the MNOS is fully turned on. At the end of the pulse the output returns to  $V_D$ . The clear operation increases the magnitude of the threshold voltage and decreases the source-drain leakage current.

Write. Writing the MNOS is similar to clearing it. However, the polarities of the pulses are reversed. The write pulse and its trigger pulse are both positive. Amplitude and pulse width are adjusted the same as for the clear pulse.

The effect of a write pulse can be seen in Fig. 13. During the write pulse there is no change in output. The positive pulse tends to turn the MNOS off rather than on. But, at the end of the pulse the transistor is turned fully on and the drain output goes momentarily to ground. This is followed by an exponential return to  $V_D$ . The reaction is caused by the large number of trapped negative charges initially



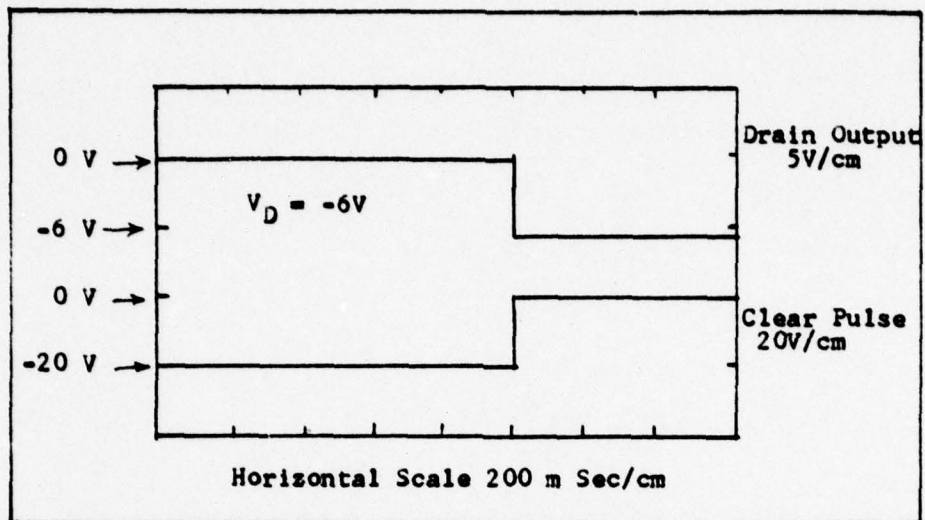


Fig. 12. Generalized Response of an MNOS to a Clear Pulse

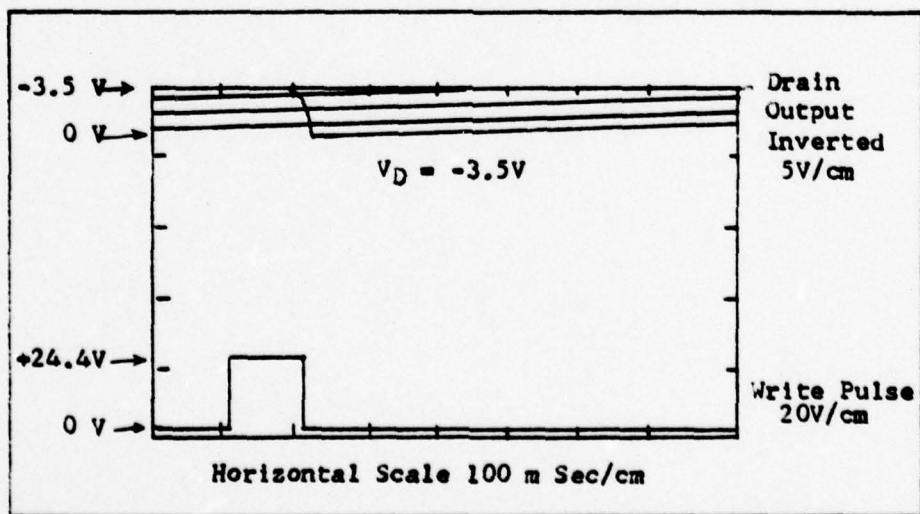


Fig. 13. Generalized Response of an MNOS to a Write Pulse

present in the nitride at the end of the write pulse. The MNOS is essentially fully turned on by its own internal fields. A large source-drain current flows until some of the charge leaks through the gate oxide. Several seconds after a saturation write pulse the leakage current returns to approximately 20 microamperes.

Reading. The final operation for which the test circuit can be used is reading. The read pulse amplitude is continuously variable from near zero to -15 volts. The power supply for the read/clear circuit has a fine voltage adjustment to permit output voltage changes of 0.01 volts.

The required trigger for the read pulse is provided by the same pulse generator which triggers the circuit for clearing an MNOS. However, for read operations the pulse-width is reduced to the minimum which will provide a clean output from the drain when threshold voltage is reached. Typically, a read pulse-width is more than two orders of magnitude less than a clear pulse-width.

For the MNOS tested in this experiment a read pulse-width of 500 microseconds is used. A shorter, 200 microseconds, pulse is adequate when  $V_T$  is small in magnitude but not when  $V_T$  approaches 10 volts. Fig. 14 shows the effect of read pulse-width on an MNOS device. The finite response time of the MNOS does not permit the shorter pulses to cause the same output as the longer pulse.

#### Experimental Method

The actual value of  $V_T$  was determined by manually varying the read pulse amplitude between pulses until an output of 0.1 volts is seen at the drain. With this circuit several attempts were usually needed to

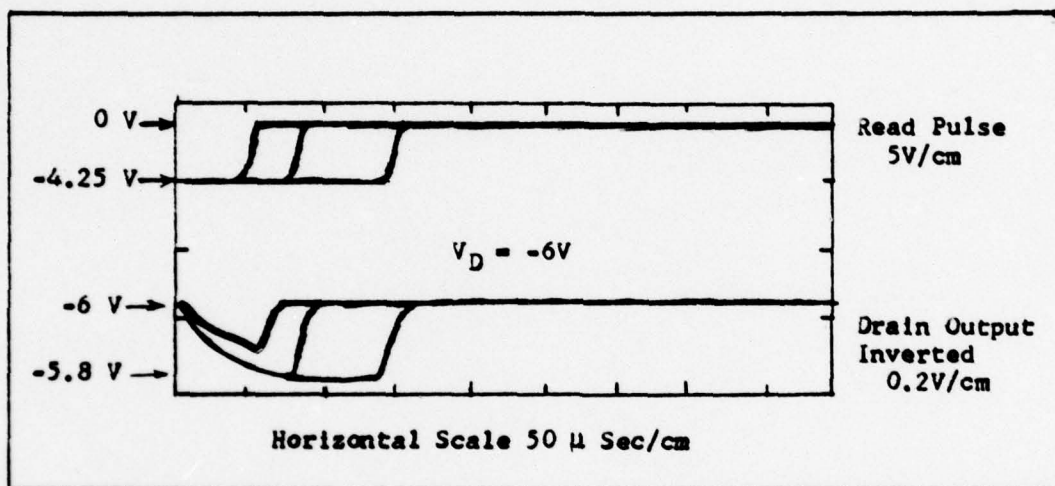


Fig. 14. Generalized Response of an MNOS to Varied Read Pulse Widths



determine the threshold voltage of an MNOS. Individual pulses were used rather than a pulse chain to minimize read-disturb effects.

Unless the approximate value of  $V_T$  was known, initial read-pulses were small in magnitude. The amplitude was increased in coarse steps until a response was first noted at the drain output. Then the read-voltage was fine adjusted to cause an output of 0.1 volts at the drain. That output voltage corresponded to threshold-voltage current across the 10K drain resistor. The drain output was monitored in the AC mode of the oscilloscope. That mode eliminated a DC voltage signal caused by the slowly varying leakage current. Once the desired output was obtained, the voltage of the read/clear power supply was read from the voltmeter and recorded as the threshold voltage.

#### Standardized Testing Procedure

Time is a critical factor in any attempt to reproduce results with an MNOS. The fact that  $V_T$  changes with time means that any value of  $V_T$  only applies at the instant at which it was determined. Therefore, any statement about threshold voltage must include information on the time history of the device.

Saturation. One convenient point for starting the time history of an MNOS is the saturate write point. The saturate write point has associated with it a fixed value of  $V_T$  for each MNOS transistor. Saturation is determined by a series of write, wait, read operations. Such a series is a write, a 15 second wait, and then a read. To accurately determine the threshold at the end of the 15 second period requires several read pulses during the waiting period. The last read

pulse, which should be at threshold voltage, should come at the end of the 15 second period.

For the MNOS used in this study, five write pulses at 25 volts with a pulse width of 1 second were used to insure saturation. Saturation has been reached when no further change in  $V_T$  occurs with additional write pulses. If desired, a single long write pulse can be used instead of the several short pulses.

Selected Threshold Voltage. A second point in time to start data on an MNOS occurs when the threshold voltage equals a set value. First a value of  $V_T$  is selected which is larger in magnitude than saturated  $V_T$ . Then the MNOS is written nearly to saturation. Finally, the device is read with pulses fixed at the selected threshold voltage amplitude. The drain output will initially be greater than 0.1 volts but will decrease to that value with time. Experiment time is started when the output reaches 0.1 volts. At that time the threshold voltage is equal to the selected threshold voltage.

#### IV. Results

To demonstrate the feasibility of an MNOS dosimeter it was necessary to show that its response to radiation was reproducible. Once that was shown, data were required concerning minimum and maximum dose and the effect of dose rate. Experimental data were therefore taken on the effect of radiation and on the effect of time on the MNOS threshold voltage. Minimal data were taken on dose-rate effects since the MNOS is considered dose-rate independent. Tallon and Vail (Ref 14) indicated that under proper test conditions the MNOS responds only to total dose effects.

##### Time Dependence

Initial tests of the variation of  $V_T$  with time indicated a logarithmic dependence. The curve in Fig. 8 shows the effects of time on  $V_T$ . The curve, on the semi-log axes, is almost linear out to the last data point at 47 hours.

A linear least squares fit applied to  $V_T$  versus  $\log_{10}$  (time) yielded a correlation coefficient of 0.98. Consequently, data on  $V_T$  versus time was only taken for approximately 30 minutes on later MNOS transistors. The threshold voltage at later points in time was estimated by extrapolation of the initial data.

Fig. 8 also shows the excellent reproducibility of the data for  $V_T$  versus time. The time history for the transistor was started from the saturation write point to insure a fixed starting value of threshold voltage.



The MNOS transistors used in this study respond slowly over time. This slow response is an asset in a device which is to be used as a dosimeter. Periods of hours are often required in experiments to achieve a large total dose.

#### Radiation and Time Dependence

The dependence of MNOS threshold voltage on the combined effects of radiation and time is shown in Fig. 15. The maximum dose shown,  $4.3 \times 10^6$  rads (Si), required 3 hours 45 minutes to accumulate. Radiation exposure was stopped at that time since the change in threshold voltage with further radiation had become minimal.

After the initial  $4.3 \times 10^6$  rads (Si) exposure, the transistor was cleared and then written again to saturation. A second radiation exposure repeated the threshold voltage measurements out to 2 M rads (Si). Further checks on reproducibility of data were made with two additional radiation exposures to 640 k rads (Si) each. The data from the first exposure were seen to differ from that of the remaining radiation exposures. The difference was determined to be a systematic error of 0.14 volts. The error was caused by failure to write the device fully into saturation prior to the start of the experiment.

After the constant 0.14 volt error was subtracted from the first set of data, the standard deviation for the data was determined. Applying a single standard deviation to the data indicated a reproducibility of  $\pm 0.01$  volts. This excellent reproducibility held for the remaining five MNOS transistors tested. The data showed such a high degree of precision,  $\pm 0.01$  volts, that discrepant values were immediately apparent.

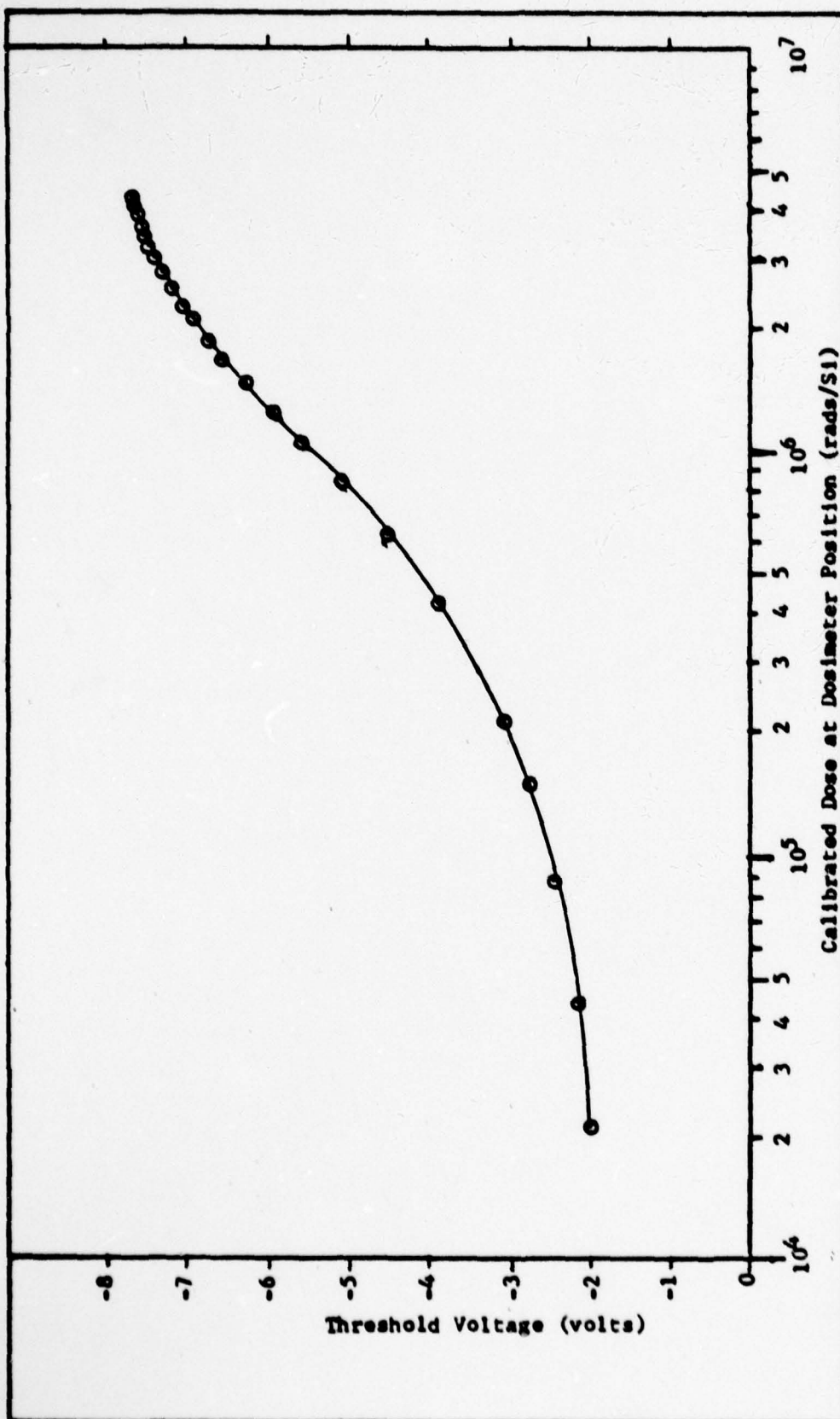


Fig. 15. Threshold Voltage Versus Calibrated Dose in Rads (Si) at Dosimeter Position

### Dosimetry Data

In order to use the MNOS as a dosimeter, the effect of radiation alone had to be separated from the previous data which included the effect of the time required for exposure to that calibrated radiation dose. Fig. 16 shows the effect of radiation alone on the value of threshold voltage. The curve shows the change in threshold voltage versus calibrated dosage for an MNOS initially written to saturation. Primary radiation effect data for the curve was obtained from a single 4.3 M rad irradiation. The first data points were then confirmed with a second irradiation to a calibrated dose of 640 k rads. After the irradiation tests, a 22 minute non-radiation test was made to determine the effects of time on the threshold voltage. The threshold voltage versus time curve was then extrapolated to provide data covering the time required to achieve the calibrated radiation dose. Then the time dependent threshold voltage data was subtracted from the radiation effect test data. Fig. 16 is the result of the subtraction.

### Theoretical Curve Fit

The suggested equation for changes in threshold voltage versus radiation, Eq (23), was fitted to the data for Fig. 16. A best value for the radiation effect constant B was found through the use of a nonlinear curve fitting computer program. With threshold voltage as the dependent variable a minimum RMS error of 0.018 yielded a value of  $B = 8.22 \times 10^{-7} \text{ rads}^{-1}$ . Fig. 16 shows the excellent agreement between the experimental and calculated data.

Although the devices tested in this study differed from the devices tested by Mariffino et al, the radiation damage constant was found to



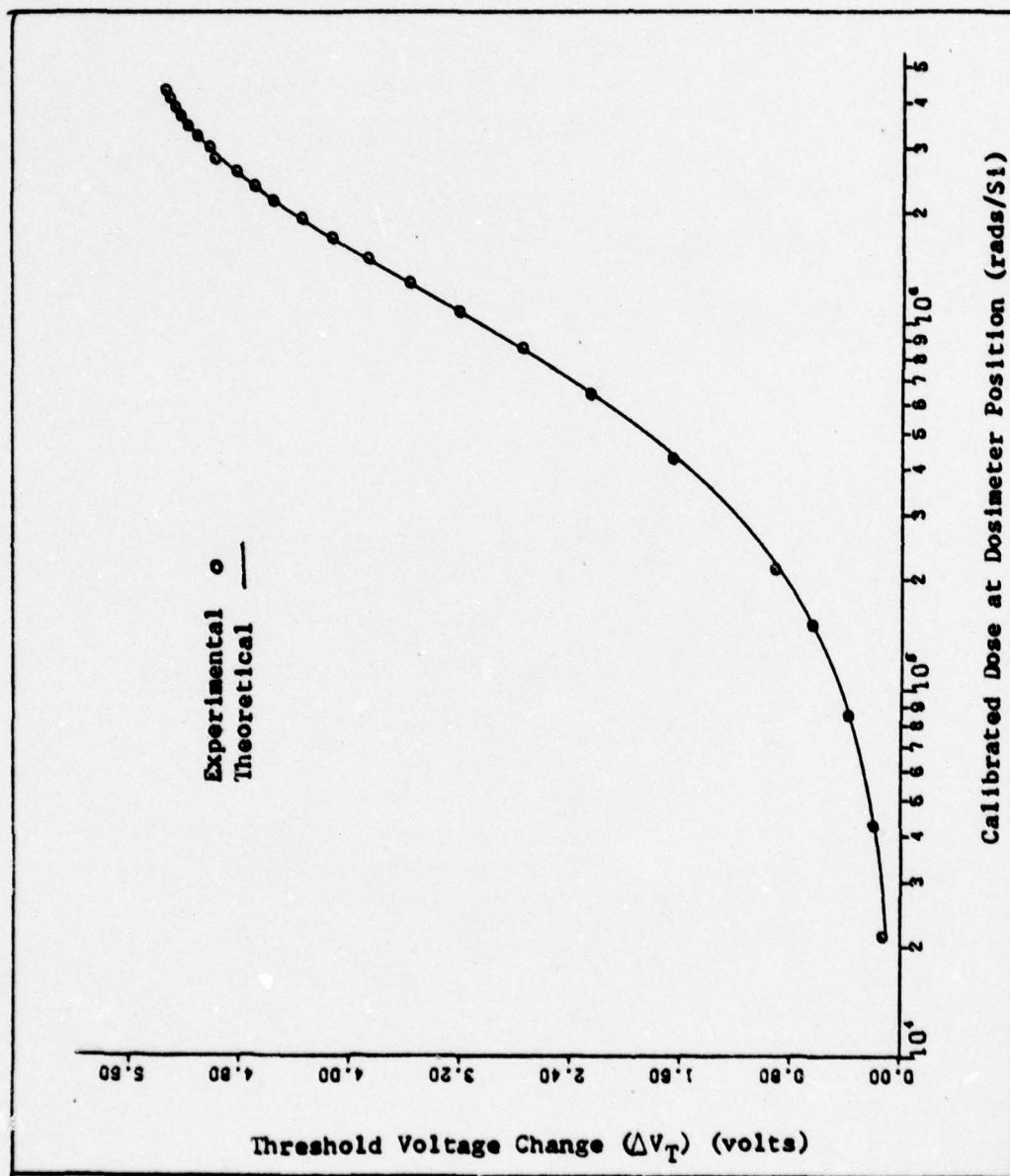


Fig. 16. Change in Threshold Voltage Versus Calibrated Dose in Rads (SI) at Dosimeter Position

be the same. The value of  $B = 8 \times 10^{-7} \text{ rads}^{-1}$  would seem to be relatively fixed for standard MNOS construction techniques.

### Precision

To determine the precision of the threshold voltage testing circuit as a dosimeter, Eq (23) was solved for radiation dose as a function of change in threshold voltage. The standard deviation in the radiation dosage was then computed using the known standard deviation of the threshold voltage measurements. Since the equation contains a logarithmic term, the precision for radiation dosage varies with the dose.

Values of the computed precision of this dosimetry method are shown in Table I. It can be seen that the precision is worst at the low dose end of the scale but improves rapidly with increased dose.

### Total Dose Effects

One MNOS device was extensively irradiated to determine if a large total dose would permanently affect it. The device was subjected to a total calibrated dose in excess of 20 M rads and showed no permanent effects. The same device was used later as a dosimeter and operated normally.

### Dosimetry

The device which was used for total radiation dose effects testing was later used to make dosimetry measurements. The average dose rate obtained from the MNOS dosimeter of  $6.42 \pm 0.08 \text{ k rads per minute}$  compared favorably with the calculated dose of  $6.5 \text{ k rads per minute}$ . The results of the dosimetry are given in Table II.

Table I  
Relative Precision of MNOS Dosimeter

Dose (Rads)	Standard Deviation (Rads)	% of Dose
21 k	$\pm 2.3$ k	11
150 k	$\pm 2.5$ k	2
213 k	$\pm 2.6$ k	1
1.9 M	$\pm 10.4$ k	0.5
4.0 M	$\pm 61$ k	1.5

Table II  
Dose Rate Calculations at Low Dose Rate

Time (Min)	$V_T$ (volts)	Time Data	$\Delta V_T$ (volts)	Dose (Rads)	Dose Rate (Rads/Min)
10	-2.12	-1.82	-.30	63.9 k	6.39 k
20	-2.45	-1.88	-.57	127 k	6.34 k
30	-2.74	-1.91	-.83	196 k	6.53 k

Table III  
Dose Rate Calculations at High Dose Rate

Run	Time (Min)	$V_T$ (volts)	Calculated Time Data (volts)	$\Delta V_T$ (volts)	Dose (Rads)	Dose Rate (Rads/Min)
1	6.26	-3.03	-1.79	-1.25	292 k	46.7 k
2	6.26	-3.04	-1.79	-1.26	292 k	46.7 k
1	10	-3.64	-1.82	-1.82	471 k	47.1 k
2	10	-3.65	-1.82	-1.83	471 k	47.1 k
1	16.22	-4.46	-1.86	-2.60	767 k	47.3 k



A second dosimetry run was made with the same device in a much higher dose rate environment. The test fixture was placed in the center of the gamma cell source array. An estimated dose for that position is 60 k rad per minute. The results of five dose calculations taken from two radiation exposures are given in Table III. The average dose obtained of  $47.0 \pm 0.2$  k rads indicates a relative precision of  $\pm 0.4\%$ .

#### Permanent Radiation Damage

After minimal testing, those transistors which had stepped gate structures showed permanent radiation effects. The typical stepped gate transistor started with an eleven volt difference between  $V_{TH}$  and  $V_{TL}$ .  $V_{TH}$  and  $V_{TL}$  are the threshold voltages in the saturated high-conduction state and the saturated low-conduction states, respectively. After a few megarads dose the value of  $V_{TH}$  had moved down to nearly the value of  $V_{TL}$ . The transistor no longer acted like an MNOS. Its characteristics were those of a fixed threshold MOS transistor.

A possible explanation of this is shown in Fig. 17. The thicker oxide on either side of the nitride layer can store charge in the same manner as an MOS transistor. The field placed on the gate and nitride layers eventually cannot overcome this excess charge. Consequently, the device no longer responds normally to write pulses. For this reason MNOS transistors with stepped gate structure cannot be used for dosimeters.

**Charge Migration.** A second permanent radiation effect was noted with these MNOS devices. When the devices were tested two weeks after their initial testing, their responses were not normal. Some would

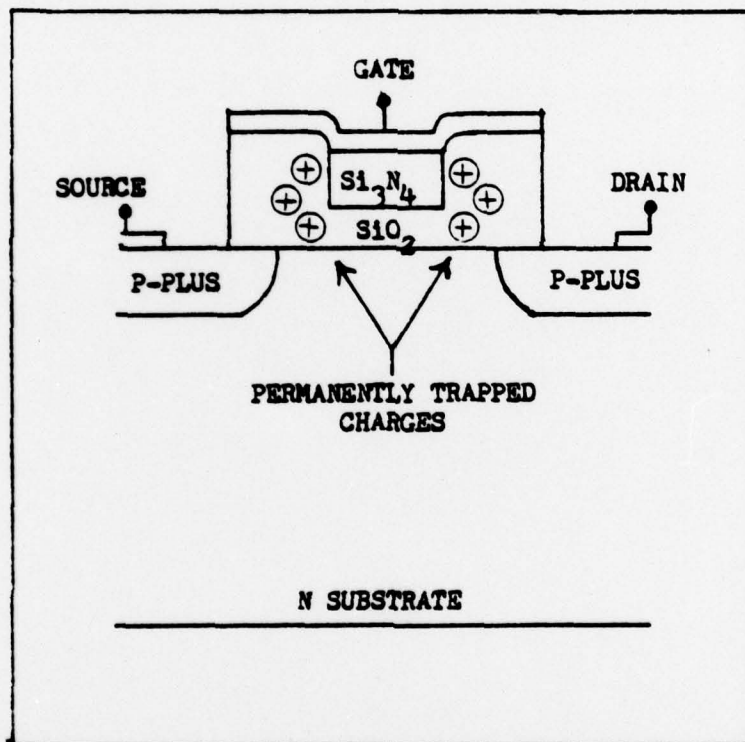


Fig. 17. Stepped Gate MNOS Showing Permanently Trapped Charges

not operate at all with the 1 M resistor in the gate circuit. For others, the response to a read pulse was a decrease in source/drain current. Such behavior was probably due to charge migration to the MNOS transistors from the remainder of the silicon chip.

The individual transistors occupied less than 1% of the total area of the chip. They were also the only circuits on the chip with connected leads. The stored charges in the MNOS transistors would have attracted any free charges which had been generated in the remainder of the large chip.

Such an effect has not been reported for discrete MNOS devices. For that reason, discrete devices are recommended for use in dosimeter applications.



## V. Conclusions and Recommendations

This chapter presents the conclusions drawn concerning the use of an MNOS as a dosimeter and recommends further work to produce an MNOS dosimeter which is fully automatic. A possible method of automatic dosimetry using an MNOS is discussed in the final section of this chapter.

### Conclusions

An MNOS transistor, used in conjunction with a simple threshold voltage detection circuit, provides the capability for high precision, high dose level dosimetry. The MNOS devices used in this study can be used to measure exposure to doses ranging from 10 k rads (Si) to more than 4 M rads (Si). Within this dose range, the relative precision is quite good. From 200 k rads (Si) to 4 M rads (Si) the relative precision is  $\pm 1\%$  of measured dose. The relative precision at low dose levels, less than 20 k rads (Si), decreases to  $\pm 11\%$  of measured dose.

Use of the MNOS dosimetry method described in this study requires determination of two different calibration curves. One calibration curve is of threshold voltage change ( $\Delta V_T$ ) versus time. The other curve is of  $\Delta V_T$  versus radiation dose. To determine a value of radiation dose, one must know both the value of  $\Delta V_T$  from saturation and the length of time of the dose. The value of  $\Delta V_T$  due to the effects of time is first subtracted from the measured  $\Delta V_T$ , and then the remaining  $\Delta V_T$  is used to determine dose from the  $\Delta V_T$  versus radiation dose curve.

MNOS transistors used for dosimetry should not have stepped-gate structures. The stepped-gate structure is like an MNOS gate with an MOS gate on either side. Under irradiation the two MOS gate sections degrade the performance of the MNOS. After sufficient dose, a few M rads (Si), the threshold voltage of the entire device is shifted to the low conduction state and can no longer be varied. Since this degradation is permanent, a stepped-gate MNOS should not be used for dosimetry purposes.

The permanent degradation by radiation of a stepped-gate MNOS also suggests problems in MNOS memory arrays. If stepped-gate devices are used, radiation damage becomes permanent. It is possible that the radiation hardness of such an array would be limited to the hardness of a comparable MOS memory array.

Radiation effects in an MNOS which cause changes in threshold voltage can be described by the equation

$$\Delta V_T = \Delta V_{TMAX} [1 - \exp(-BR)] \quad (24)$$

where  $\Delta V_T$  is the change in threshold voltage,  $\Delta V_{TMAX}$  is the maximum change in threshold voltage, B is an experimentally determined constant ( $\text{rads}^{-1}$ ), and R is the total dose in rads. The value for B determined for one of the devices in this study is  $8.22 \times 10^{-7}$ . This value corresponds to a value of  $8 \times 10^{-7}$  found by Marriffino, et al (Ref 12:18).

The use of MNOS devices which were part of a large MNOS test chip lead to permanent degradation of the MNOS devices. A probable cause for this damage is charge migration from the remainder of the large test chip to the MNOS transistors. Because of this effect, MNOS devices for dosimetry should be discrete transistors if possible.

### Recommendations

The final portion of this study involved an attempt to design a partially automatic dosimetry method. One requirement for full automation is an automatic threshold voltage detection circuit. Analog circuits exist for this task, but the inherent accuracy of a digital circuit is desired.

The block diagram of a suggested circuit is shown in Fig. 18. A circuit using that block diagram was breadboarded and given very limited testing. It was not always able to reproduce measurements to 0.01 volts, and there was insufficient time to fully study the circuit. Much further work is needed to determine best design and test such a circuit for precision of measurement.

Further study is also recommended into the use of the MNOS dosimeter in other radiation environments. There is evidence that the MNOS is relatively insensitive to neutron effects (Ref 5). An MNOS dosimeter might therefore be able to measure gamma radiation in a reactor environment.

A final step in the development of an MNOS dosimeter would be to couple an automatic threshold voltage reader to a small microprocessor. The microprocessor could store the data on both threshold voltage versus dose and threshold voltage versus time, monitor the dosimetry runs, and provide an automatic digital read out of dose.



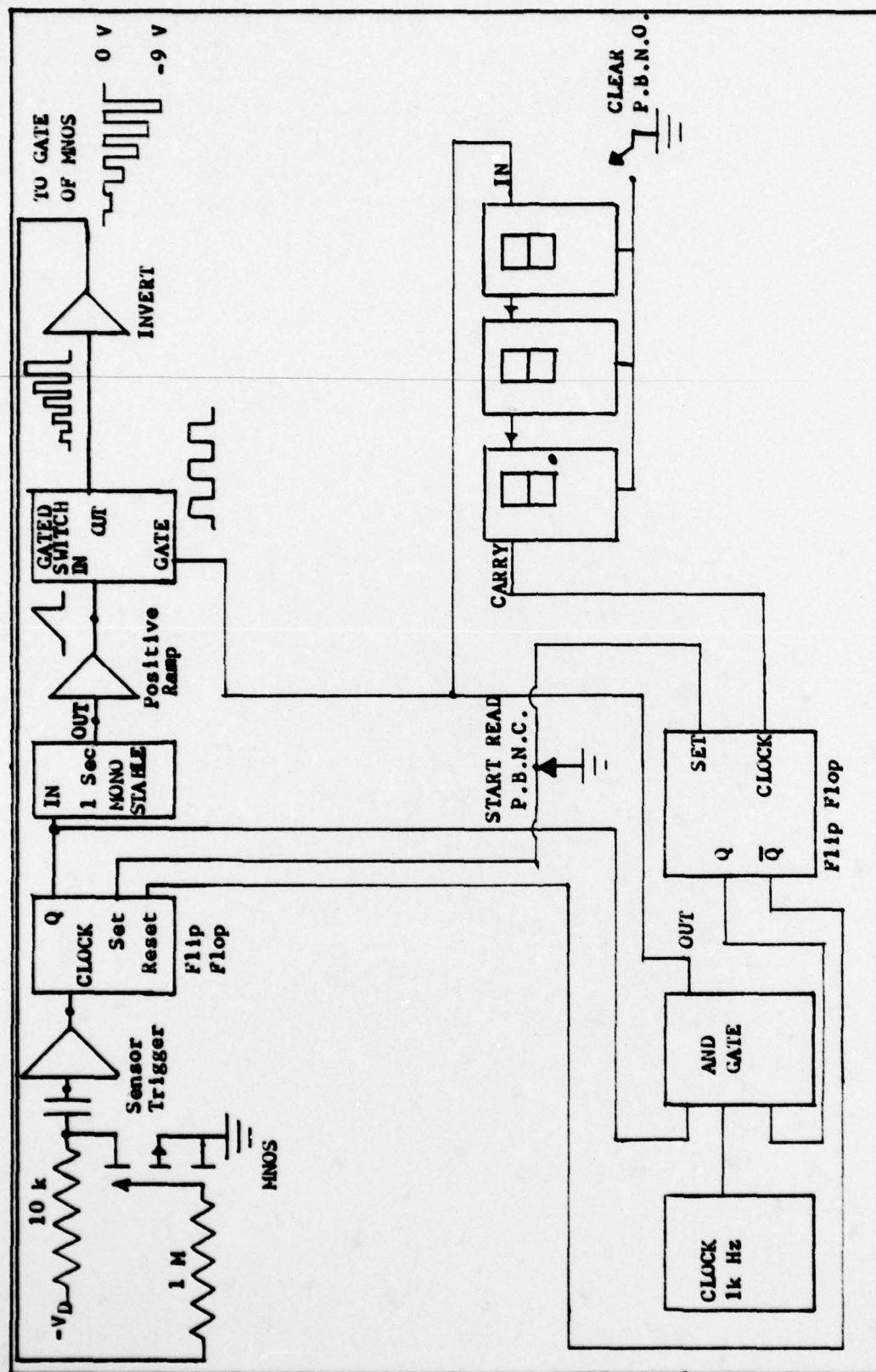


**Fig. 18. Block Diagram of Automatic Threshold Voltage Measurement Circuit**

### Bibliography

1. "A New Use for MOS Transistors: to Detect Accumulated Radiation." Electronic Design, 11:32 (May 27, 1971).
2. Bentchkowsky, D. F. "The Metal-Nitride-Oxide-Silicon (MNOS) Transistor - Characteristics and Applications." Proceedings of the IEEE, 58:1207-1219 (August 1970).
3. Church, V. E., et al. "Direct Readout Instrument for Gamma Dosimetry." Scientific Instruments, March 1976, pp. 182-186.
4. Ciarlo, D. R., et al. "Metal-Oxide-Semiconductor X-Ray Detectors." IEEE Transactions on Nuclear Science, NS-19:350-355 (February 1972).
5. Giril, V. A., et al. "Effect of Neutron Radiation and Gamma Radiation on the Parameters of Metal-Insulator-Semiconductor Structures." Soviet Atomic Energy, 35:663-664 (July 1973).
6. Gregory, B. L. and C. W. Gwyn. "Radiation Effects on Semiconductor Devices." Proceedings of the IEEE, 62:1264-1273 (September 1974).
7. Holm, N. W. and R. J. Berry. Manual on Radiation Dosimetry. New York: Marcel Dekker, Inc., 1970.
8. Knoll, M. "MNOS Dosimeter." Proposed Thesis Topic. Air Force Weapons Laboratory, Kirtland AFB, New Mexico. May 1977.
9. Lundstrom, K. I. and C. M. Svensson. "Properties of MNOS Structures." Transactions on Electron Devices, ED-19:826-836 (June 1972).
10. Preliminary Standards for MNOS Transistor Characteristics to be published. Produced by the IEEE MNOS Standardization Subgroup in 1974.
11. Snow, E. H., et al. "Effects of Ionizing Radiation on Oxidized Silicon Surfaces and Planar Devices." Proceedings of the IEEE, 55:1168-1185 (July 1967).
12. Sperry Gyroscope. Design and Fabrication of Radiation-Hardened MNOS Memory Array. AFWL-TR-74-209. Great Neck, New York: Sperry Rand Corporation, July 1975.

13. Svensson, C. M. and K. I. Lundstrom. "Trap Assisted Charge Injection in MNOS Structures." Journal of Applied Physics, 44:4657-4663 (October 1973).
14. Tallon, R. W. and D. J. Vail. "A Comparison of High Dose Rate Test Results on MNOS Transistors in E-Beam and Gamma Environments." Unpublished. Air Force Weapons Laboratory, Kirtland AFB, New Mexico. December 1974.



## VITA

Ronald Guy Fraass was born on 13 March 1948 in Lincoln, Nebraska. He graduated from high school in Mankato, Kansas in 1966 and attended Kansas State University from which he received the degree of Bachelor of Science, Nuclear Engineering, in December 1970. Upon graduation, he received a commission in the USAF through the ROTC program. He immediately entered active duty and completed pilot training in December 1971. He served initially as a Search and Rescue Pilot with the 76th Aerospace Rescue and Recovery Squadron, Hickam AFB, Hawaii. He then served as a C-130 pilot in the 39th Tactical Airlift Squadron, Pope AFB, North Carolina until entering the School of Engineering, Air Force Institute of Technology, in August 1976.

Permanent address: 113 North High Street  
Mankato, Kansas 66956

This thesis was typed by Frances Jarnagin.

UNCLASSIFIED

SECURITY CLASSIFICATION OF THIS PAGE (When Data Entered)

REPORT DOCUMENTATION PAGE		READ INSTRUCTIONS BEFORE COMPLETING FORM
1. REPORT NUMBER <b>AFIT/GNE/PH/78M-3</b>	2. GOVT ACCESSION NO.	3. RECIPIENT'S CATALOG NUMBER <b>Master's thesis</b>
4. TITLE (and Subtitle) <b>USE OF A METAL-NITRIDE-OXIDE-SEMICONDUCTOR AS THE DETECTOR FOR A RADIATION DOSIMETER.</b>		5. TYPE OF REPORT & PERIOD COVERED <b>MS Thesis</b>
7. AUTHOR(s) <b>RONALD FRAASS</b> <i>Guy</i>		6. PERFORMING ORG. REPORT NUMBER
9. PERFORMING ORGANIZATION NAME AND ADDRESS <b>Air Force Institute of Technology (AFIT-EN) Wright-Patterson AFB, Ohio 45433</b>		8. CONTRACT OR GRANT NUMBER(s)
11. CONTROLLING OFFICE NAME AND ADDRESS <b>Transient Radiation Effects Branch (AFWL/ELT) Air Force Weapons Laboratory Kirtland Air Force Base, NM</b>		10. PROGRAM ELEMENT, PROJECT, TASK AREA & WORK UNIT NUMBERS <b>12 58P.</b>
14. MONITORING AGENCY NAME & ADDRESS (if different from Controlling Office)		12. REPORT DATE <b>Mar 1978</b>
		13. NUMBER OF PAGES <b>55</b>
		15. SECURITY CLASS. (of this report) <b>Unclassified</b>
		15a. DECLASSIFICATION/DOWNGRADING SCHEDULE
16. DISTRIBUTION STATEMENT (of this Report)  <b>Approved for public release; distribution unlimited</b>		
17. DISTRIBUTION STATEMENT (of the abstract entered in Block 20, if different from Report)		
18. SUPPLEMENTARY NOTES  <b>Approved for public release; IAW AFR 190-17</b>  <i>Jerral F. Guess</i> <b>JERRAL F. GUESS, Captain, USAF Director of Information</b>		
19. KEY WORDS (Continue on reverse side if necessary and identify by block number) <b>MNOS Dosimeter, Dosimetry Metal-Nitride-Oxide-Semiconductor Radiation Effects</b>		
20. ABSTRACT (Continue on reverse side if necessary and identify by block number) <b>A method of radiation dosimetry using a Metal-Nitride-Oxide-Semiconductor (MNOS) device as the detector was developed and partially evaluated. The MNOS devices are capable of measuring doses from 10 k rads to 4 M rads. Repeatability of observations indicates a precision of <math>\pm 1\%</math> of total dose from 200 k rads to 4M rads (Si). Dosage in rads is obtained by reference to a calibrated source exposure rate and not to dose absorbed within the dosimeter. A <math>\text{Co}^{60}</math> source was used for all radiation testing. Schematics are given for some of the circuits tested. Determination of dosage from the system is indirect and</b>		

DD FORM 1 JAN 73 1473

EDITION OF 1 NOV 65 IS OBSOLETE

UNCLASSIFIED

SECURITY CLASSIFICATION OF THIS PAGE (When Data Entered)

012 225

LW

UNCLASSIFIED

SECURITY CLASSIFICATION OF THIS PAGE(When Data Entered)

Continuation of Block 20. ABSTRACT

requires the use of a calibration curve. Each dosimeter must be calibrated from a known source. Direct readout of dose is suggested by use of a micro-processor. Exposure to  $2 \times 10^5$  rads did not degrade performance. Devices eventually failed due to charge migration from the large integrated circuit chip on which they were fabricated. Discrete, non-stepped gate MNOS transistors are recommended.

2000000000

UNCLASSIFIED

SECURITY CLASSIFICATION OF THIS PAGE(When Data Entered)